JOURNAL OF THE ROYAL LAUREATES ACADEMY

www.rlaindia.org

# PERFORMANCE ANALYSIS OF A DOUBLE-PASS SOLAR AIR HEATER INTEGRATED WITH A WATER-BASED THERMAL STORAGE SYSTEM

**Khoob Singh**

Research Scholar, Department Arni School of Technology, Arni University, Himachal Pradesh, India

**Dr. Sanjay Yadav**

Professor, Department Arni School of Technology, Arni University, Himachal Pradesh, India

## ABSTARCT

The purpose of the experimental setup is to investigate the effects of different operating conditions on the heat transfer efficiency of a water-based thermal storage system connected with a double-pass solar air heater. Inside this system, you'll find a solar air heater with a glass cover, an insulated mild steel frame, and a selectively coated copper absorber. A centrifugal blower supplies regulated airflow via a directed tunnel. The conventional flat absorber is replaced with an integrated thermal storage medium consisting of twelve copper pipes filled with water and connected by copper plates. This allows for greater energy retention. The air is heated twice in a sequence, once in the upper channel and once in the lower channel, before exiting the system. We measure temperature, mass flow rate, and sunlight intensity using calibrated thermocouples, a sun meter, and flow meters. Sustainable heat supply is tested by charging and discharging at different mass flow rates to measure thermal efficiency, temperature rise, and overall system performance.

**Keywords:** Solar, Thermal, Storage, Efficiency, Performance.

## I. INTRODUCTION

Sustainable and affordable, solar air heaters (SAHs) are becoming more popular for their ability to transform solar radiation into heat. Space heating, crop drying, industrial heating, and ventilation systems are just a few of the many thermal applications in which they are crucial. Traditional single-pass solar air heaters are simple to construct, but they have a poor thermal efficiency because the air traveling over the absorber surface does not transmit enough heat to the air. To overcome this constraint and increase heat transfer performance, energy storage capabilities, and overall system dependability, researchers have been exploring new configurations and novel additions. The DPSAH is a highly efficient design that has been suggested among several operational and geometrical adjustments. Because it allows air to flow over and under the absorber plate, increasing the heat transfer area, the DPSAH beats conventional systems in terms of thermal performance. One big issue with solar air heaters is that their heat production is unpredictable and only happens sometimes. Temperatures at the air exit are not static since solar radiation varies with the seasons, the time of day, and the sun's location. For applications requiring a steady supply of heat, this limitation becomes a major nuisance. Adding thermal energy storage (TES) devices to SAHs is one way to address this issue. In order to maintain a consistent temperature, thermal storage devices may take in excess heat while the sun is shining brightly and let it out when the light isn't so bright. Among the several TES options that are now available, such as phase change materials, packed beds, and pebble storage, water-based thermal storage stands out due to its high specific heat capacity, low cost, non-toxicity, and availability. The capacity of water to retain large quantities of heat without undergoing phase shift would be a significant boon to solar heating systems that need heat retention for brief durations or between day and night.

Combining a double-pass solar air heater with a water-based thermal storage system introduces a hybrid approach to thermal management. Streamlining energy collecting and discharge activities is achieved by this integration. Here, heated air transfers some of its energy to water or other water-based media, functioning as a dynamic heat sink. It is possible to utilize this stored energy to maintain warm air production during periods of low radiation, such as the late afternoon or overcast weather. By combining the thermal storage system with the double-pass design, the SAH is able to extend its operating efficiency window, improve temperature stability, and lower system losses. The addition of water-based TES, which allows the system to heat both water and air, greatly

increases its adaptability and practicality in both commercial and residential settings. There has been a recent uptick in interest in hybrid solar thermal systems, which integrate air heaters with heat storage components. Research shows that double-pass configurations outperform single-pass systems because to greater turbulence, longer air residency length, and improved absorber plate-air contact. By including thermal storage components such as water reservoirs, paraffin wax, or rock beds, the overall thermal efficiency of the system is substantially improved. The use of water in TES systems is especially advantageous since it reduces thermal stratification, distributes heat evenly, and causes less material damage. Water is ideal for maintaining consistent air temperatures, which are necessary for crop drying, heating greenhouses, and industrial preheating systems.

In order to comprehend the operational features, efficiency patterns, and thermal behavior of a DPSAH coupled with a water-based thermal storage system, it is crucial to conduct a performance study of the system. To find out whether these integrated systems can withstand real-world climate conditions, we measure things like temperature increase, thermal efficiency, pressure drop, heat retention, and discharge characteristics. Performance study also sheds light on the system's internal heat transfer and thermodynamic processes, such as how the moving air interacts with the thermal storage medium. Taking the time to evaluate these factors helps with optimization and also paves the way for more reliable and flexible solutions. Hybrid systems, such as the DPSAH with an integrated water-based TES, have the ability to significantly improve the usage of sustainable thermal energy, which is particularly promising in light of the growing need for renewable energy solutions throughout the world and the growing focus on energy conservation. These systems provide practical and affordable options for both rural and industrial areas, reducing reliance on traditional heating sources and greenhouse gas emissions. To find out what factors affect performance, how much efficiency is gained, and how to put it into practice, a thorough performance study is necessary in this case. This work contributes to the advancement of solar thermal technology by offering comprehensive understanding about how water-based thermal storage might improve the efficiency of double-pass solar air heaters.

## II. LITERATURE REVIEW

Patel, Vimalkumar. (2023). to improve the efficiency of the device's energy transmission from the heart to other parts of the device, the solar air heater is connected with a device called a double pass solar air heater (DPSAH). They claim that single-pass solar air heaters don't create as much thermal energy as those with many passes because they lose some of the energy during the transfer process. However, due to its energy-efficient design, DPSAH achieves improved thermal efficiency, which is reflected in its superior thermal efficiency. This is achieved by increasing the area of heat transmission. An important part of a DPSAH's solar energy collecting system is the absorber plate, which sits behind the collector and soaks up the sun's rays. It is common practice to paint it black in order to increase solar energy absorption since this hue directly affects the growth of larger absorption. The use of recycled materials in the building of the absorber plate and the subsequent efficiency would presumably be part of the investigation. Remember that organic or inorganic dyes or semiconductors make up the vast majority of absorber materials used for this application.

Ismail, Amar et al., (2022) Double-pass solar air thermal collectors are investigated in this study using porous lava rock as a substrate. Because of its short-term heat storing properties, lava rock is an ideal component of a sun drying system. A higher convective heat transfer rate to the airflow is a result of both increased turbulence in the air channel and an increase in the heat transfer area. To tackle energy balance issues quantitatively, a mathematical model was constructed in MATLAB. Scientists varied the wind speeds and sun intensities to assess the collector's thermal performance, which they achieved by adjusting the three design parameters: collector size, air mass flow rate, and lava rock volume. In terms of flow rate, the optimal range was determined to be 0.035 kg/s and intensity to be between 62% and 64%, with a sweet spot for efficiency between 500 W/m² and 800 W/m². A porosity of around 89% was found to be optimal for the collector after considering pressure drop and thermal efficiency. A temperature output range of 41.7 to 48.3 °C was optimal for agricultural and food drying applications. Meanwhile, it was found that, on average, DPSAHs using lava rock had a 17.5% higher increase in output temperature than standard DPSAHs.

Baig, Wajahat & Ali, Hafiz. (2019) There were four different setups that were experimentally

investigated for the purpose of implementing a double pass solar air heater. This study examines the use of paraffin wax as a thermal storage medium in conjunction with aluminum, a porous/foam metal, for use in cold weather applications. The experiment began with a flat plate as the first creation, and the second setup included inserting two copper conduits with foam aluminum and paraffin wax into them. In the third configuration, four copper ducts were used. For the second phase of the experiment, the same sets were used, but this time, they were pre-heated. Although the heat conductivity was enhanced in configurations two and three, wax could not be melted in air temperatures ranging from twelve to twenty-four degrees Celsius. When the surrounding air temperature was 15–29 °C, the wax melted with the help of pre-heat. While foam aluminum improved heat conductivity, it reduced the storage capacity of paraffin wax somewhat. Prior to this configuration, wax was melted all day long under the same conditions without using a fan. The third and second variations only provided timely heat for 1.5 hours after dusk, however the fourth configuration continued to provide 2.5 hours of usable heat.

Mohammed, Akeel. (2016) even though the building can be heated throughout the day using the extra heat from the solar air heater, it will need additional heat after dark. This study aims to construct and test two-pass solar air heaters (SAHs) that can store extra solar energy and release it after sunset. Without thermal energy storage (water), and with it, the SAHs will undergo testing. Experiments were conducted in January 2016 to compare the effects of different air mass flow rates and cold winter days on the solar air heater's daytime performance while water was stored. Experimental results showed that a mass flow rate of 0.04 kg/s resulted in an average efficiency of 65% for the double pass method without optimization and 83% for the same method with optimization. By increasing the air mass flow rate, we were able to decrease the collector's temperature gain and boost its efficiency. When using water as thermal storage, the maximum temperature differential between the incoming and outgoing airflows is 30°C at a mass flow rate of 0.03 kg/s. A three-hour period after sunset saw an average air temperature 7.6 °C greater than the input temperature, according to the study. This disparity was caused by the water acting as a thermal storage medium at the absorber plate.

Ramani, Bharat et al., (2010) Adding a porous substance to the second air passage of a double-pass counterblow solar air collector is a great way to improve thermal performance, which is a very desired design improvement. This paper presents a theoretical and experimental analysis of

two solar air collector types: one with and one without a porous component. The volumetric heat transfer coefficient was essential in the development of this mathematical model. We have discussed how several variables impact the thermal performance and pressure drop characteristics. Thermodynamic efficiency is 30–35% more in the first case, and 20–25% higher in the second, when contrasted with single pass and double pass solar air collectors devoid of porous absorbing material, respectively.

Ganeshkumar, Poongavanam et al., (2021) By integrating shot blasting and winglets into the air path, the DPSAH offers a feasible design enhancement for excellent thermal performance without breaking the bank. Three different absorber plate configurations for DPSAHs were tested experimentally: (a) V-corrugation with shot blasting, (b) V-corrugation with shot blasting and a 4-3 winglet pattern, and (c) V-corrugation with shot blasting and a 3-2 winglet pattern. Further, to enhance heat transfer performance via channel turbulence, aluminum winglets are soldered to the DPSAH absorber plate. Both the wingless and winged DPSAHs had their pressure drop and thermal performance measured at regular intervals using meteorological data such outside temperature, wind speed, solar irradiation, and inside temperature. The highest pressure drop for V-corrugation with 4-3 winglets is 230 Pa and the thermal efficiency is 49.5% at a mass flow rate of 0.02 m/s. The findings showed that the thermal efficiency might be as high as 7% higher when comparing the V-corrugation air heater to one with 4-3 winglets. Finally, increasing the mass flow rate from 0.01 kg/s to 0.02 kg/s results in a pressure loss that is 1.22 times for V-corrugation and 1.3 times for V-corrugation with 4-3 winglets. In addition, there is a comprehensive economic study of DPSAHs in relation to India.

## III. EXPERIMENTAL SET-UP AND EQUIPMENT:

### Testbed Configuration:

Photographs of the experimental setup are available in plates (1) and (2) for this inquiry. An electric centrifugal blower (1 kW, 1600 rpm) supplies the air heater with air on a continual basis. Air is drawn in from the atmosphere by means of an electrical centrifugal blower and thereafter conveyed to the SAH via a tunnel. A network of tunnel-based guiding vanes uniformly disperses air over the air heater's width. As for the internal measurements, SAH is 2 × 1 × 0.16. You can see through the 4 mm thick glass that covers the top of the SAH. Eight millimeters separate the

absorber plate and glass cover. There is a gap of around eight cm between the back plate and the absorber plate. The air heater's structure is made of 1.7 mm thick mild steel plate. To improve solar radiation absorption and decrease heat loss between the inside and outside surfaces, a selective coating black layer ($\alpha = 0.93$, $\varepsilon = 0.30$) is applied to the upper surface of the 2.00 m long, 1.05 m wide, and 0.6 mm thick copper absorber plate.

As it passes through the gap between the absorber plate and the transparent glass cover, the air is first heated. The air moves counterclockwise in the bottom channel. Between the absorber and the rear plate, the air is heated to an even higher temperature. Insulating the system with 0.06 m of glass wool on both the sides and the bottom reduces heat losses to the ambient air. The whole solar air heater is oriented south and tilted 46 degrees from the horizontal for maximum sun radiation absorption.

To improve the system's performance, twelve 5 cm x 200 cm x 0.15 cm copper pipes are used in place of the conventional absorber flat plate to store the excess thermal energy. There are copper plates that go between the pipe spaces. The dimensions of each plate are $200 \times 5 \times 0.06$ cm³. To maximize solar radiation absorption and minimize energy loss, copper plates and pipes are coated selectively. A gate valve connects the air heater's input to the blower. The gate valve and an air flow meter may be used to regulate the mass flow rate of air. The temperatures of the air entering and exiting the system, the absorber plate, the glass, and the back plate were all monitored by attaching various K-type thermocouples to the digital data recorder. A solar meter is used to measure the intensity of the sun's beams. The details of the measurement tools are shown in Table-1. For the double-pass solar air heater, the experimental setup is shown in plate (2) using the thermal storage material.

**Table 1: Instrument-Specific Accuracy Levels and Error Profiles**

| Instrument | Accuracy | Range |
|---|---|---|
| K-type thermocouple | 0.3% | −110°C ~ 1250°C |
| AT45xx Multi-channel Temperature Meter | 0.3% + 1°C | −190°C ~ 1700°C |

| | | |
|---|---|---|
| Solar power meter | 4% | 0 ~ 2100 W/m² |
| Air flow meter | 1.2% | 0.3 ~ 42.0 m/s |

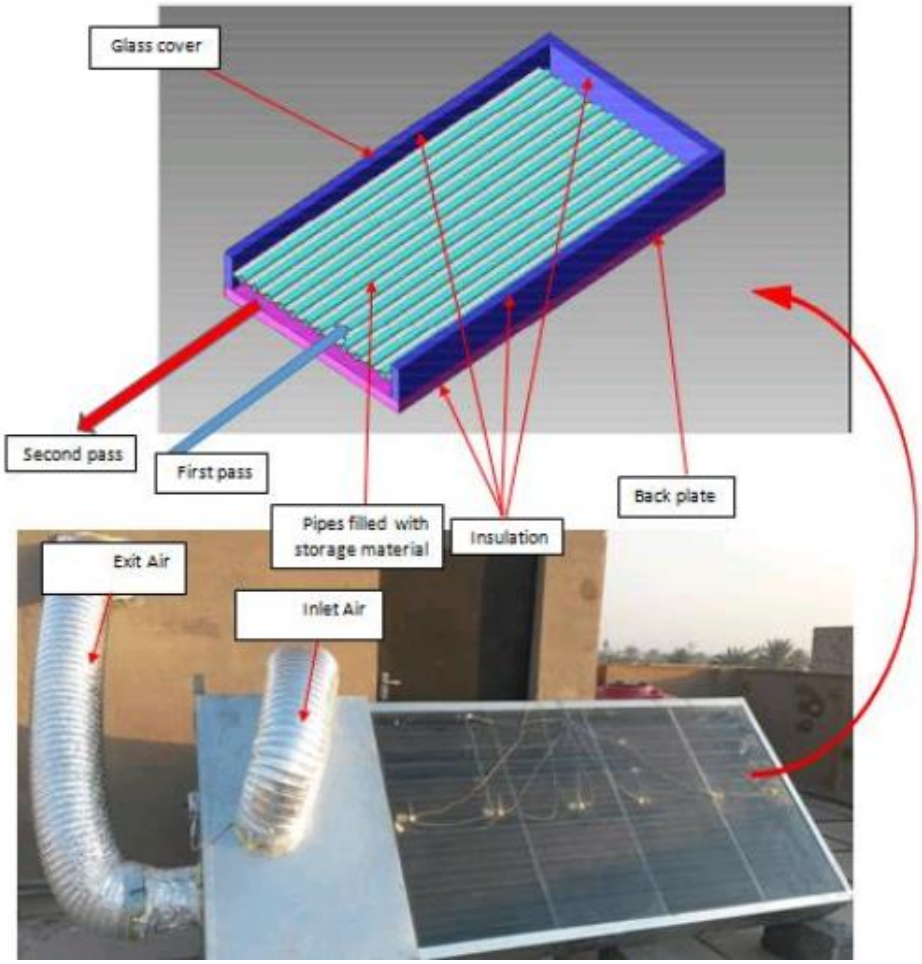


**Figure 1: Enhanced Double-Pass Solar Air Heater Utilizing Thermal Storage**

**Experimental trials:**

Under varying air mass flow rates, the system's performance is assessed by charging and discharging trials, both with and without a PCM thermal storage unit. Throughout the day, the radiation strength and air temperatures that enter and exit the solar collector are recorded at 10-minute intervals. The intake is filled with outside air so that experiments involving charging and discharging may be conducted. Methods use mass flow rates between 0.03-0.05 kg/s. Multiple

tests are performed to ensure that the readings can be reliably reproduced.

## IV. RESULTS AND DISCUSSION

### The system performance with thermal storage:

Figure 1 shows the results from the January 2016 investigations, which indicate the variation of solar insolation. The chart shows that solar insolation increases from 200 W/ at 8:00 AM to around 725 W/ at 12:00 PM. Solar insolation decreases when this window closes until sunset, which occurs around 5 o'clock in the afternoon.

**Table 1: Solar Radiation Data for Different Days**

| Time of Day (hrs) | 28th Jan. 2016 ($W/m^2$) | 29th Jan. 2016 ($W/m^2$) | 30th Jan. 2016 ($W/m^2$) |
|---|---|---|---|
| 8:00 AM | 100 | 120 | 110 |
| 9:00 AM | 250 | 280 | 260 |
| 10:00 AM | 450 | 470 | 460 |
| 11:00 AM | 600 | 630 | 610 |
| 12:00 PM | 700 | 750 | 740 |
| 1:00 PM | 750 | 780 | 760 |
| 2:00 PM | 700 | 710 | 700 |
| 3:00 PM | 550 | 570 | 560 |
| 4:00 PM | 400 | 430 | 420 |
| 5:00 PM | 250 | 270 | 260 |
| 6:00 PM | 150 | 170 | 160 |
| 7:00 PM | 50 | 60 | 55 |

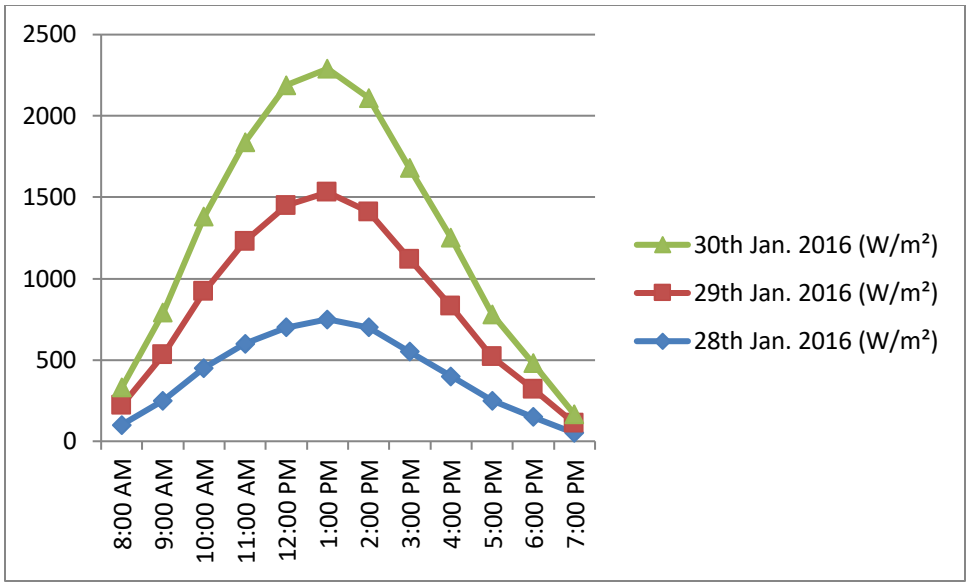


**Figure 1: Solar Radiation Data for Different Days**

The solar radiation's hourly fluctuation over three days in a row (January 28, 29, and 30, 2016) is shown in Table 1. Sun radiation follows the usual diurnal pattern, rising steadily in the morning until midday and then gradually falling in the late afternoon and evening, according to the statistics. During all three days, the sun's radiation starts to climb after dawn, although at a relatively low level around 8:00 AM, ranging from 100 to 120 W/m². At 10:00 AM, the radiation levels reach 450-470 W/m², showing a dramatic increase in solar availability due to the sun's ascent in the sky. Midday is the most efficient time to catch solar energy since that's when the radiation is at its peak, between 12:00 and 1:00 PM, when values reach 700-780 W/m². Radiation levels drop down sharply around 1 p.m. when the sun dips lower in the sky. Values fall to 400–430 W/m² by 4:00 PM, and then to 50–60 W/m² by 7:00 PM, which is a very low point. On all three days, the trend has been downward, which indicates that the atmosphere is steady and not subject to abrupt changes caused by clouds or other weather disturbances. Looking at the radiation levels from all three days, we can see that January 29th consistently had somewhat higher readings than the other two. This might be because the sky was cleaner or there was less air scattering on that day. Values for the 28th and 30th of January are quite comparable, with just little changes, most likely caused by the same weather.

**Table 2: Temperature Variation of SAHWS on 29th January 2016**

| Time of Day (hrs) | Te (Inlet Temperature, K) | Tu (Upper Plate Temperature, K) | Tw (Water Temperature, K) | Tl (Outlet Temperature, K) |
|---|---|---|---|---|
| 8:00 AM | 290 | 290 | 290 | 290 |
| 9:00 AM | 300 | 310 | 305 | 300 |
| 10:00 AM | 310 | 320 | 315 | 310 |
| 11:00 AM | 320 | 330 | 325 | 320 |
| 12:00 PM | 330 | 340 | 335 | 330 |
| 1:00 PM | 335 | 345 | 340 | 335 |
| 2:00 PM | 330 | 340 | 335 | 330 |
| 3:00 PM | 320 | 330 | 325 | 320 |
| 4:00 PM | 310 | 320 | 315 | 310 |
| 5:00 PM | 300 | 310 | 305 | 300 |
| 6:00 PM | 295 | 305 | 300 | 295 |
| 7:00 PM | 290 | 300 | 295 | 290 |

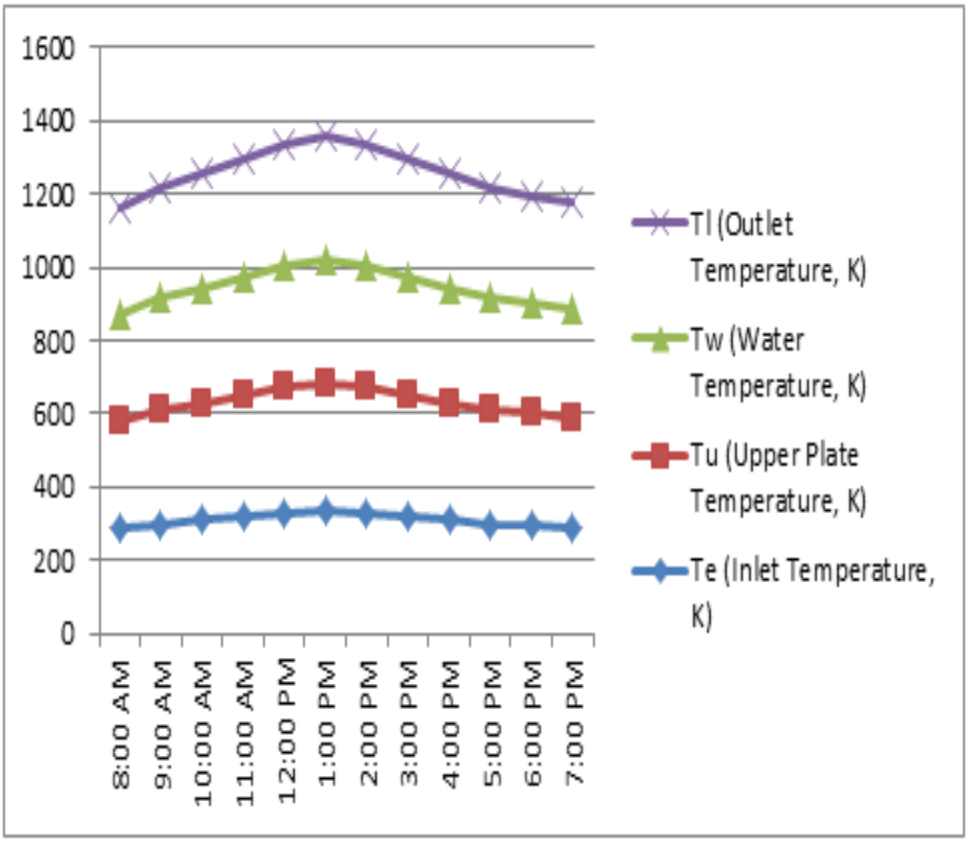


**Figure 2: Temperature Variation of SAHWS on 29th January 2016**

See how the various parts of the Solar Air Heating and Water Storage (SAHWS) system changed in temperature during the day on January 29, 2016, as shown in Table 2. Among these temperatures are those of the air entering the system, the air leaving it, the water, and the top plate. The statistics show that the system's thermal behavior is affected by solar radiation and absorbs heat throughout the day. At eight in the morning, all temperatures are the same at 290 K, suggesting that the weather is consistent before the sun comes out. The sun's rays get more intense during the day, causing temperatures to climb gradually. From 9:00 AM to 1:00 PM, there is a notable rise in the upper plate temperature (Tu), which goes from 310 K to 345 K. Because it absorbs and transforms solar radiation into thermal energy, the absorber plate exhibits a robust reaction to solar heating, as seen by this consistent increase. Around 1:00 PM, the water temperature (Tw) reaches 340 K, indicating that there is efficient heat transmission from the collector to the water storage medium. This trend continues throughout the day. Just like the entrance temperature pattern, the output air temperature (Tl) rises and peaks at 335 K somewhere between noon and early afternoon. As a result of changes

in the surrounding air temperature and gains in system heat, the intake temperature (Te) increases somewhat. The progressive drop in all temperature readings after 1:00 PM is a reflection of the sun's waning strength. At four in the afternoon, the temperature drops to about 310–320 K, and by seven in the afternoon, it's back to the baseline from the morning, with Tu slightly higher at 300 K because of the absorber surface's residual heat.

**Table 3: Estimated Air Temperature Gradient ($T_o - T_i$) Under Varying Mass Flow Rates for the Double-Pass SAHWS**

| Time of Day | m = 0.03 kg/s | m = 0.04 kg/s | m = 0.045 kg/s | m = 0.05 kg/s |
|---|---|---|---|---|
| 8:00 AM | 2 | 3 | 3 | 4 |
| 9:00 AM | 8 | 10 | 11 | 12 |
| 10:00 AM | 15 | 18 | 19 | 20 |
| 11:00 AM | 22 | 26 | 27 | 28 |
| 12:00 PM | 28 | 33 | 34 | 35 |
| 1:00 PM | 30 | 36 | 37 | 38 |
| 2:00 PM | 31 | 37 | 38 | 39 |
| 3:00 PM | 30 | 36 | 37 | 38 |
| 4:00 PM | 25 | 31 | 32 | 33 |
| 5:00 PM | 18 | 24 | 25 | 26 |
| 6:00 PM | 10 | 14 | 15 | 16 |
| 7:00 PM | 4 | 6 | 7 | 7 |
| 8:00 PM | 1 | 2 | 2 | 3 |

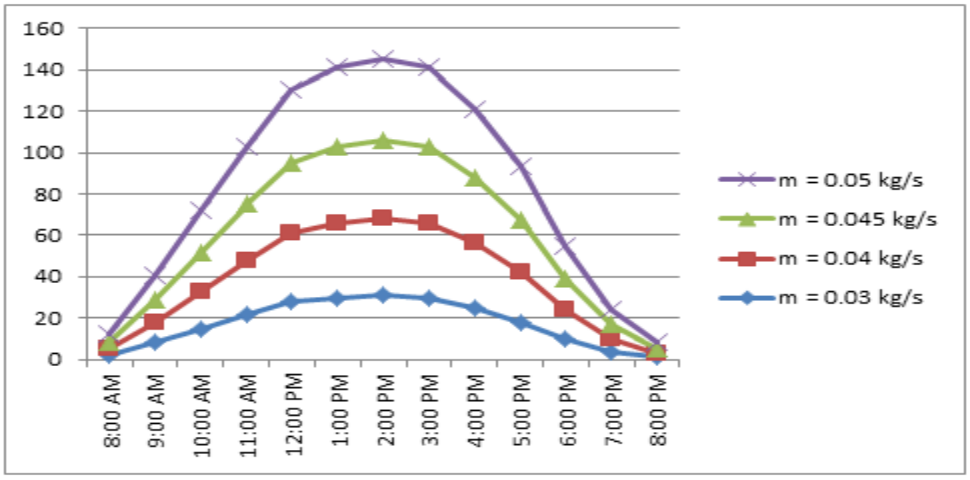


**Figure 3: Estimated Air Temperature Differential ($T_o$ – $T_i$) Across Various Mass Flow Rates in a Double-Pass SAHWS**

The air temperature difference ($T_o$ - $T^k$) varies under four various mass flow rates for a double-pass Solar Air Heating and Water Storage (SAHWS) system, as shown in Table 3. As a measure of the system's efficiency in transferring heat from the absorber plate to the air passing over it, the temperature difference is a crucial metric for practical heat gain. With the rising light intensity and thermal energy availability, the temperature difference increases at all mass flow rates between dawn and midday. During the early hours of sunlight, the findings are at their lowest around 8:00 AM, with temperature changes of 2 to 4°C, indicating that there is very little heating. The temperature differential grows sharply as the sun's rays intensify, reaching its maximum between one and two in the afternoon. There is considerable heat transfer performance during peak sun exposure, as the temperature differential approaches 38-39°C at greater mass flow rates during these hours. It becomes evident that there is a tendency whereby temperature disparities are regularly bigger at increasing mass flow rates. An example of this would be the temperature gradient from 28°C at 0.03 kg/s to 35°C at 0.05 kg/s at noon. It may be inferred that a higher airflow rate improves convective heat transfer, leading to a greater heat extraction from the absorber surface. At peak hours, the gap between 0.045 kg/s and 0.05 kg/s narrows, indicating a slow but steady approach to thermal saturation, beyond which increasing the flow rate causes declining returns. The disparity in temperatures narrows as the sun sets and the day draws to a close. The numbers fall to almost nothing by 7:00 or 8:00 PM, which means that the system can't heat as much since the sun isn't shining as brightly.

**Table 4: Hourly Useful Heat Gain (W) at Different Mass Flow Rates**

| Time of Day | m = 0.03 kg/s | m = 0.04 kg/s | m = 0.045 kg/s | m = 0.05 kg/s |
|---|---|---|---|---|
| 8:00 AM | 50 | 60 | 55 | 40 |
| 9:00 AM | 150 | 180 | 200 | 130 |
| 10:00 AM | 350 | 420 | 480 | 310 |
| 11:00 AM | 650 | 700 | 850 | 550 |
| 12:00 PM | 800 | 900 | 1000 | 750 |
| 1:00 PM | 820 | 950 | 1050 | 700 |
| 2:00 PM | 830 | 930 | 1000 | 650 |
| 3:00 PM | 820 | 850 | 900 | 500 |
| 4:00 PM | 700 | 780 | 820 | 400 |
| 5:00 PM | 500 | 600 | 650 | 300 |
| 6:00 PM | 300 | 350 | 400 | 150 |
| 7:00 PM | 150 | 180 | 200 | 80 |
| 8:00 PM | 80 | 90 | 100 | 40 |

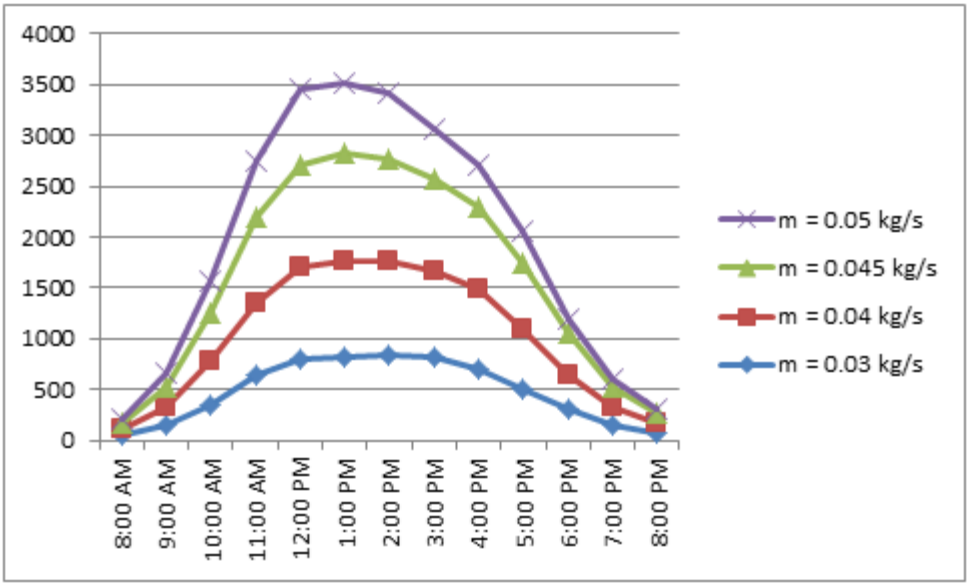


**Figure 4: Useful Heat Gain (W) Across Varying Mass Flow Rates Throughout the Day**

Table 4 displays the solar air heater's usable heat gain at various mass flow rates throughout a day. These numbers show how well the system works under different situations to transform solar energy into heat. Both the time of day and the mass flow rate seem to have a significant impact on the overall pattern. At 8:00 AM, all mass flow rates start to experience relatively modest levels of usable heat gain, which ranges from 40 to 60 W. Heat gain increases dramatically with rising sun radiation. By midday, the system's thermal performance has increased to 1000 W at 0.045 kg/s, a significant improvement from 9:00 AM to 12:00 PM. The heating window is at its most efficient at this time since it coincides with when the sun is at its strongest. There is an ideal trade-off between heat transfer and air residence time at 0.045 kg/s, which consistently yields the maximum beneficial heat gain among all mass flow rates. Performance is modest at lower flow rates, and significantly decreased at the maximum flow rate (0.05 kg/s) throughout the day. This decrease at 0.05 kg/s demonstrates the drawbacks of high mass flow, which may shorten the air-to-plate contact time and therefore the amount of heat that can be absorbed. The ideal flow rate range has a substantial heat gain of 900 to 1050 W between noon and two o'clock in the afternoon. As the sun sets, the performance starts to drop after 2:00 PM. Depending on the flow rate, heat gain lowers to 400–820 W by 4:00 PM, and it drops even more to 40–100 W by 7:00–8:00 PM in the evening.

**Table 5: Temporal Variation of Air Temperature Difference During the Discharge Phase**

| Time of Day | m = 0.03 kg/s | m = 0.04 kg/s | m = 0.045 kg/s |
|---|---|---|---|
| 4:30 PM | 17 | 13 | 10 |
| 5:00 PM | 12 | 9 | 6 |
| 5:30 PM | 9 | 7 | 4 |
| 6:00 PM | 7 | 5 | 3 |
| 6:30 PM | 5 | 4 | 2.5 |
| 7:00 PM | 3.5 | 2.5 | 2 |
| 7:30 PM | 2 | 1 | — (approx. 0) |

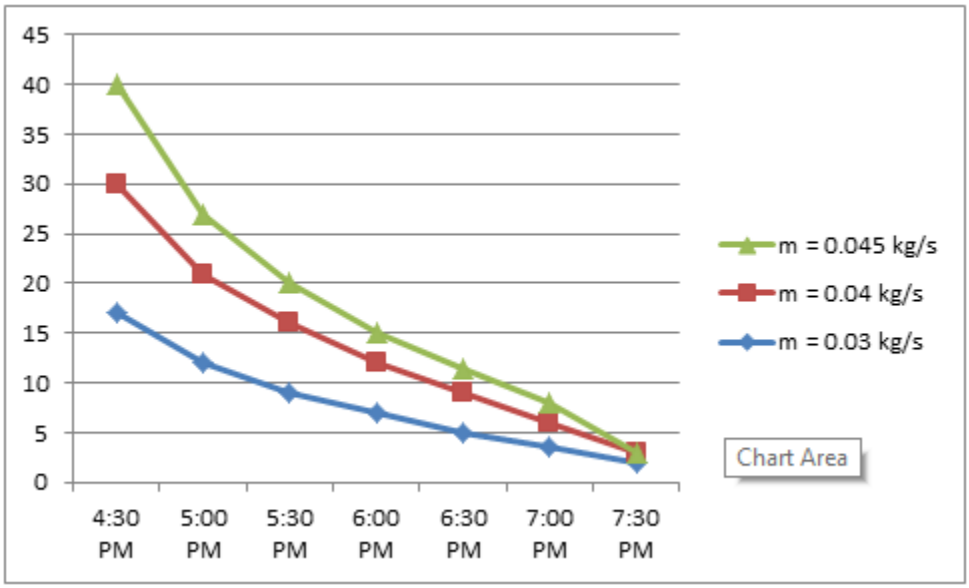


**Figure 5: Air Temperature Difference as a Function of Standard Local Time During the Discharge Phase**

For three distinct mass flow rates, Table 5 shows how the air temperature differential ($T_{□}$ - $T^{k}$) changed during the discharge time. During the discharge phase, thermal energy is slowly released from storage after the peak of solar radiation. As the night wears on, the statistics show that the temperature difference decreases, which is a reflection of the heat that has been stored. The discharge period's temperature differences reach their peak around 4:30 PM, when residual solar heat is still quite high, with values of 17°C at 0.03 kg/s, 13°C at 0.04 kg/s, and 10°C at 0.045 kg/s. What this means is that before cooling starts, the system releases a lot of thermal energy that it has accumulated. Higher flow rates are associated with smaller temperature increases because quicker air movement removes heat more rapidly, as seen by the lower temperature differential at these rates. Regardless of the flow rate, the temperature differential reduces consistently as the day draws to a close. There is a dramatic decrease in accessible thermal energy by 6:00 PM, as the values for the three flow rates fall to 7°C, 5°C, and 3°C, respectively. As the sun goes down, heat storage decreases and solar input drops as well, leading to this scenario. Temperature variations are rather small, from 1-3.5°C, between 7:00 and 7:30 PM in the late evening. The temperature differential approaches zero at 0.045 kg/s at 7:30 PM, signaling that all useful stored heat has been used up and that the system has returned to ambient temperature.

**Table 6: Thermal Efficiency as a Function of Mass Flow Rate Across the Day**

| Time of Day | m = 0.03 kg/s | m = 0.04 kg/s | m = 0.045 kg/s | m = 0.05 kg/s |
|---|---|---|---|---|
| 8:00 AM | 0.05 | 0.05 | 0.06 | 0.04 |
| 9:00 AM | 0.15 | 0.18 | 0.20 | 0.13 |
| 10:00 AM | 0.30 | 0.33 | 0.35 | 0.25 |
| 11:00 AM | 0.42 | 0.46 | 0.48 | 0.38 |
| 12:00 PM | 0.50 | 0.55 | 0.58 | 0.45 |
| 1:00 PM | 0.55 | 0.60 | 0.63 | 0.50 |
| 2:00 PM | 0.60 | 0.67 | 0.70 | 0.55 |

| | | | | |
|---|---|---|---|---|
| 3:00 PM | 0.70 | 0.78 | 0.82 | 0.65 |
| 4:00 PM | 0.85 | 0.93 | 1.00 | 0.80 |
| 4:30 PM | 1.00 | 1.10 | 1.20 | 0.95 |
| 5:00 PM | 1.25 | 1.35 | 1.45 | 1.10 |
| 5:30 PM | 1.55 | 1.65 | 1.75 | 1.40 |
| 6:00 PM | 1.80 | 1.90 | 2.00 | 1.70 |

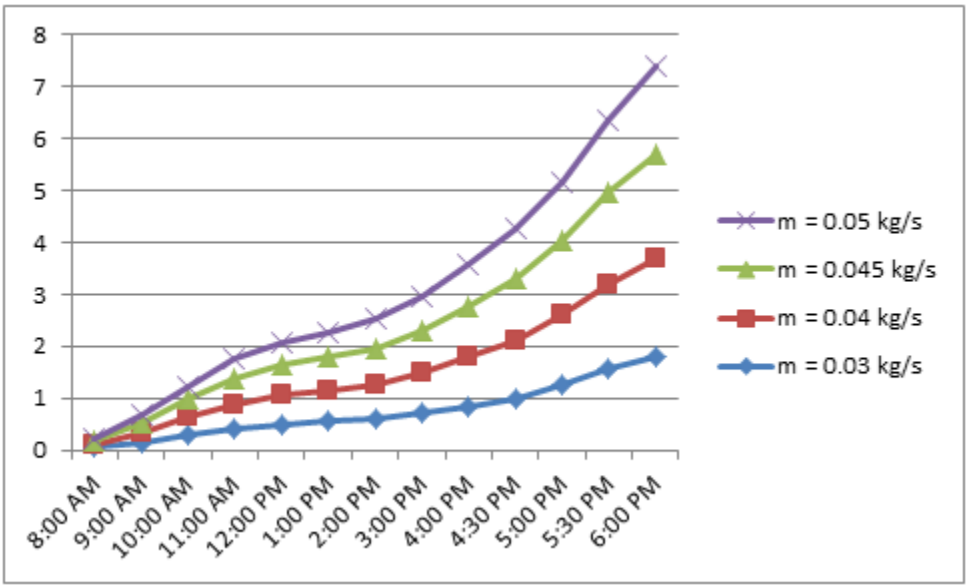


**Figure 6: Thermal Efficiency as Influenced by Mass Flow Rate Throughout the Day**

Table 6 shows the thermal efficiency of the solar air heater at different mass flow rates throughout the day, along with a link between sun intensity, operating conditions, and system performance. Over the course of a day, thermal efficiency increases consistently due to improved heat transmission, system stability, and the rising sun. The morning hours of 8:00 to 10:00 are characterized by persistently low thermal efficiency, with mass flow rates ranging from 0.04 to 0.35. Since the system is still far from reaching its optimal operating temperature and solar radiation is weak, this is to be expected. Efficiency is at its peak during the hours of 10:00 AM and

2:00 PM, when the sun's rays are at their strongest. This time period's efficiency ranges from 0.30 to 0.70 for different mass flow rates, indicating a good thermal interaction between the absorber surface and the airflow and a high level of heat absorption. Higher mass flow rates, and more especially 0.045 kg/s, always provide the best efficiency. The optimal airflow velocity to heat transfer surface contact ratio, as shown by this pattern, is 0.8. Assuming declining returns due to insufficient air residence time in the heating channel, efficiency is fair at lower mass flow rates (0.03 kg/s) but drops off drastically at the maximum mass flow rate (0.05 kg/s). Values between 1.00 and 1.20, achieved between 3:00 and 4:30 in the afternoon, indicate optimal efficiency. The system is functioning at peak efficiency when all three conditions are met: a constant absorber temperature, gentle airflow, and complete usage of stored thermal energy. At a flow rate of 0.045 kg/s, efficiency achieves its maximum of 2.00 between 5:30 and 6:00 in the afternoon. Improving performance immediately before sunset is due to releasing stored thermal energy and reducing thermal losses induced by colder surroundings.

## V. CONCLUSION

The integration of a water-based thermal storage system into a double-pass solar air heater represents a significant advancement in solar thermal technology. The hybrid configuration effectively addresses key limitations of conventional solar air heaters by enhancing heat transfer, improving energy storage capability, and ensuring stable thermal output even during fluctuating solar radiation conditions. The double-pass design increases the contact surface area and residence time of air, allowing for more efficient heat absorption, while the water-based TES acts as a reliable buffer that stores surplus energy and releases it when needed. This combination not only improves overall thermal efficiency but also enhances system versatility and reliability across diverse applications. Performance analysis results demonstrate that such integrated systems can maintain higher temperature differentials, achieve improved exergy levels, and reduce thermal losses compared to conventional designs. Moreover, water’s high specific heat capacity ensures effective short-term heat retention, making the system suitable for agricultural, residential, and industrial heating requirements. As renewable energy technologies continue to evolve, hybrid solar air heaters with thermal storage will play an increasingly important role in sustainable energy utilization. This study reinforces the potential of DPSAH systems and provides a foundation for further innovations aimed at maximizing solar thermal efficiency and operational stability

**REFERENCES:**

**[1]** K. I. Al-Chlaihawi, B. H. Alyas, and A. A. Badr, "CFD based numerical performance assessment of a solar air heater duct roughened by transverse-trapezoidal sectioned ribs," *Int. J. Heat Technol.*, vol. 41, no. 5, pp. 1273–1281, 2023.

**[2]** N. F. Hussein, S. T. Ahmed, and A. L. Ekaid, "Thermal performance of double pass solar air heater with tubular solar absorber," *Int. J. Renew. Energy Dev.*, vol. 12, no. 1, pp. 11–21, 2023.

**[3]** Patel, V., "Performance Evaluation of a Double-Pass Solar Air Heater with Recycled Materials as Absorber Plate," *IJSRD – Int. J. Sci. Res. Dev.*, vol. 11, no. 6, pp. 1–8, 2023.

**[4]** Ismail, A., A. S. Abd Hamid, A. Ibrahim, H. Jarimi, and K. Sopian, "Performance analysis of a double pass solar air thermal collector with porous media using lava rock," *Energies*, vol. 15, no. 3, pp. 905–912, 2022.

**[5]** H. Yaseen, M. Özalp, and W. Khalil, "Second law analysis of double pass solar air heater equipped with aluminum recycled cans as augmentation techniques," M.S. thesis, Dept. Mech. Eng., Karabuk Univ., Turkey, 2022.

**[6]** S. Panda and R. Kumar, "A review on heat transfer enhancement of solar air heater using various artificial roughened geometries," *J. Adv. Res. Fluid Mech. Therm. Sci.*, vol. 89, no. 1, pp. 92–133, 2022.

**[7]** B. K. Roomi and M. A. Theeb, "Experimental and numerical study of inserting an internal hollow core to finned helical coil tube-shell heat exchanger," *J. Eng. Sustain. Dev.*, vol. 25, no. 1, pp. 1–14, 2021.

**[8]** G. Raju and M. M. J. Kumar, "Experimental study on solar air heater with encapsulated phase change material on its absorber plate," *Energy Storage*, vol. 3, no. 5, pp. 1–16, 2021.

**[9]** Ganeshkumar, P., S. Duraisamy, B. Kumar, M. Salman, and S. Kim, "Performance enhancement of a double-pass solar air heater with a shot-blasted absorber plate and winglets," *J. Mech. Sci. Technol.*, vol. 35, no. 2, pp. 1–9, 2021.

**[10]** A. S. Abdullah *et al.*, "Experimental investigation of single pass solar air heater with reflectors and turbulators," *Alexandria Eng. J.*, vol. 59, no. 2, pp. 579–587, 2020.

**[11]** T. K. Abdelkader *et al.*, "Energy and exergy analysis of a flat-plate solar air heater artificially roughened and coated with a novel solar selective coating," *Energies*, vol. 13, no. 4, pp. 1–22, 2020.

**[12]** Z. Alabdeen H. Obaid, A. Al-damook, and W. H. Khalil, "The thermal and economic characteristics of solar air collectors with different delta turbulators arrangement," *Heat Transf. – Asian Res.*, vol. 48, no. 6, pp. 2082–2104, 2019.

**[13]** Baig, W., and H. Ali, "An experimental investigation of performance of a double pass solar air heater with foam aluminum thermal storage medium," *Case Stud. Therm. Eng.*, vol. 14, no. 1, 100440, 2019.

**[14]** A. S. Mahmood, "Experimental study on double-pass solar air heater with and without using phase change material," *J. Eng.*, vol. 25, no. 2, pp. 1–17, 2019.

**[15]** M. Aktaş *et al.*, "Energy-exergy analysis of a novel multi-pass solar air collector with perforated fins," *Int. J. Renew. Energy Dev.*, vol. 8, no. 1, pp. 47–55, 2019.

**[16]** F. Chabane, N. Moummi, and A. Brima, "Experimental study of thermal efficiency of a solar air heater with an irregularity element on absorber plate," *Int. J. Heat Technol.*, vol. 36, no. 3, pp. 855–860, 2018.

**[17]** B. Varun Kumar *et al.*, "A performance evaluation of a solar air heater using different shaped ribs mounted on the absorber plate—A review," *Energies*, vol. 11, no. 11, pp. 1–26, 2018.

**[18]** Mohammed, A., "Experimental Performance Evaluation of a Double Pass Solar Air Heater With and Without Thermal Storage," *Aust. J. Basic Appl. Sci.*, vol. 10, no. 16, pp. 138–148, 2016.

**[19]** A. S. Ali, A. I. Bhatti, and M. Ali, "An experimental investigation of performance of a double pass solar air heater with thermal storage medium," *Therm. Sci.*, vol. 19, no. 5, pp. 1699–1708, 2015.

**[20]** R. Pandey and M. Kumar, "Efficiencies assessment of an indoor designed solar air heater characterized by V-baffle blocks having staggered racetrack-shaped perforation geometry," *Sustain. Energy Technol. Assess.*, vol. 47, p. 101362, 2021.

**[21]** Ramani, B., A. Gupta, and R. Kumar, "Performance of a double pass solar air collector," *Solar Energy*, vol. 84, no. 11, pp. 1929–1937, 2010.

**[22]** A. Saxena and V. Goel, "Solar air heaters with thermal heat storages," *Chin. J. Eng.*, vol. 2013, pp. 1–11, 2013.

**[23]** H. F. Oztop, F. Bayrak, and A. Hepbasli, "Energetic and exergetic aspects of solar air heating (solar collector) systems," *Renew. Sustain. Energy Rev.*, vol. 21, pp. 59–83, 2013.